Spin frustration and an exotic critical point in ferromagnets from nonuniform opposite g factors

Weiguo Yin ,* Christopher R. Roth, and Alexei M. Tsvelik

Condensed Matter Physics and Materials Science Division, Brookhaven National Laboratory, Upton, New York 11973, USA

(Received 5 December 2023; accepted 7 February 2024; published 26 February 2024)

It is demonstrated that novel spin frustration can be induced in ferromagnets with nonuniform opposite Landé g factors. The frustrated state is characterized by a mutual interplay of typical ferromagnetic (FM) and antiferromagnetic (AFM) features, such as the zero-field susceptibility being FM-like at low temperatures but AFM-like at high temperatures. It is also found to contain an exotic zero-temperature "half fire, half ice" critical point at which the spins on one sublattice are fully disordered and on the other one are fully ordered. We suggest that such frustration may occur in a number of copper-iridium oxides such as Sr_3CuIrO_6. We also anticipate a realization of the frustration and "partial fire, partial ice" states in certain antiferromagnets, lattice gas, and neuron systems.

DOI: 10.1103/PhysRevB.109.054427

I. INTRODUCTION

Frustrated magnets are known to give rise to exotic magnetic states such as spin ice, spin glass, and spin liquid that may play important roles in quantum computing, spintronics, and unconventional superconductivity [1–8]. The essence of frustration is usually assumed to be ground-state degeneracy that emerges as a consequence of competing exchange interactions among the spins. Such frustration demands that some or all of the exchange interactions be antiferromagnetic (AFM) [Figs. 1(a) and 1(b)], or in case the exchange interactions are all ferromagnetic (FM), that they have strong direction-dependent anisotropy [Fig. 1(c)] [3,4]. Recently, there has been an intense search for frustrated magnetism beyond the "standard model" of condensed matter physics [2,9–14].

Here, we suggest a different mechanism of frustration, the one which can exist in magnets with uniform FM exchange interactions and is related to the nonuniformity of the Landé g factors. It is likely to exist in a family of copper-iridium oxides such as $(\mathrm{Sr,Ba})_{2+n}\mathrm{CuIr}_n\mathrm{O}_{3n+3}$ ($n =$ 1–4), $Ba_9Cu_2Ir_5O_{21}$, $Ba_{14}Cu_3Ir_8O_{33}$, and $Ba_{16}Cu_3Ir_{10}O_{39}$ [15–20]. The copper oxides and the iridium oxides themselves are respectively the most extensively studied $3d$ and $5d$ transition-metal compounds (TMCs) for a wide range of topics from frustrated magnetism to high-temperature superconductivity; thus, it has been of great interest to study the mixed copper-iridium oxides. A critical unresolved problem in this field is that Sr_3CuIrO_6, the parent compound long believed to be an isotropic spin one-half ($S = \frac{1}{2}$) chain ferromagnet [19–21], displays a strange spin glassy behavior with zero-field susceptibility being FM- and AFM-like at low and high temperatures, respectively [15]. These observations seemed to suggest the existence of substantial AFM exchange interactions [15–18], but a recent first-principles symmetry analysis and resonant inelastic x-ray scattering experiments have reestablished the uniform FM nature of the effective exchange interactions in Sr_3CuIrO_6—with a strong Ising-like anisotropy [22,23]. We hereby point to a largely unnoticed difference in the characters of the $3d$ and $5d$ TMCs, namely their g factors are usually positive and negative, respectively; thus, the most outstanding character of the copper-iridium oxides is the unusual alternation of the g factors [Fig. 1(d)]. As shown in Sec. II, it is the different combinations of spin-orbit coupling and crystal-field splitting for the $3d$ and $5d$ ions that make the g factors strongly site dependent, viz., $g \approx 2$ and -3 for the Cu and Ir sites, respectively, along the easy axis. Below we use the Ising chain model to rigorously demonstrate that such a disparity in the g factors does generate strong frustration in both zero-field and critical-field limits. Since the Ising model is one of the basic models in statistical mechanics and condensed matter physics [24] having been applied even to explain the activity of neurons in the brain [25], we anticipate the present results to be widely applicable.

II. STAGGERED g FACTORS ($-g_{\mathrm{Ir}} > g_{\mathrm{Cu}} > 0$) IN THE COPPER-IRIDIUM OXIDES

Both the orbital angular momentum (**L**) and spin angular momentum (**S**) of an electron contribute to the magnetic moment ($\mathbf{M}_J$) in the following form,

$$\begin{aligned}\mathbf{M}_J &= \mathbf{M}_L + \mathbf{M}_S,\\ \mathbf{M}_L &= g_L\mu_B\mathbf{L},\\ \mathbf{M}_S &= g_S\mu_B\mathbf{S},\end{aligned} \tag{1}$$

where in atomic physics, $g_L = 1$ and $g_S = 2$. However, a strong octahedral crystal field will split the d orbitals into the well-separated e_g and t_{2g} energy levels. The t_{2g}^5 subsystem such as Ir^{4+} in the copper-iridium oxide Sr_3CuIrO_6 can be transformed to an effective $L = 1$ system [22,23]—upon projecting out the unoccupied e_g levels—in which $|xy, \sigma\rangle$ and $i|yz, \sigma\rangle \pm |zx, \sigma\rangle$ (where $\sigma = \uparrow$ or $\downarrow$ is the spin index) are the

*wyin@bnl.gov

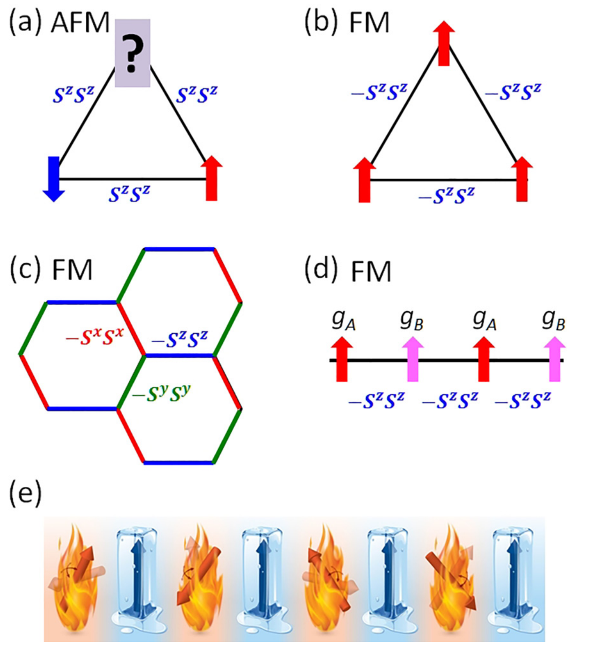

FIG. 1. (a) Frustrated spins on triangular lattice with AFM interactions. (b) Unfrustrated spins for FM interactions. (c) Frustrated spins on a honeycomb lattice with FM interactions whose anisotropic axes are bond dependent [3,4]. (d) Spins in a chain with uniform FM interactions and alternating g factors ($-g_B > g_A > 0$) are found frustrated. (e) A cartoon illustration of the half fire, half ice critical point at which the spins on one sublattice are fully disordered and on the other are fully ordered.

new $L_z = 0$ and ± 1 states, respectively, with [26]

$$g_L = -1. \tag{2}$$

Then, strong spin-orbit coupling on the Ir atom generates an effective total angular momentum $J = \frac{1}{2}$ state [22].

The g-factor tensor that relates the total magnetic moment $\mathbf{M}_J$ and the total angular momentum $\mathbf{J} = \mathbf{L} + \mathbf{S}$ is given by

$$\langle J, J_z|\mathbf{M}_J|J, J_{z'}\rangle = g_J^{z,z'} \mu_B \langle J, J_z|\mathbf{J}|J, J_{z'}\rangle, \tag{3}$$

where the effective $J = \frac{1}{2}$ wave vectors $|J, J_z\rangle$ for Ir atoms in Sr_3CuIrO_6 are given by [22]

$$\left|J, \pm\frac{1}{2}\right\rangle = \frac{1}{\sqrt{p^2+2}}[p|xy, \uparrow\rangle + i|yz, \downarrow\rangle \pm |zx, \downarrow\rangle], \tag{4}$$

where $p \approx 0.65$. Hence the longitudinal g factor that couples to the magnetic field along the z direction is

$$\begin{aligned} g_{\mathrm{Ir}}^z = g_J^{z,z} &= \frac{\langle J, \frac{1}{2}|M_z|J, \frac{1}{2}\rangle}{\mu_B\langle J, \frac{1}{2}|J_z|J, \frac{1}{2}\rangle} \\ &= 2\left\langle J, \frac{1}{2}\middle|g_L L_z + g_S S_z\middle|J, \frac{1}{2}\right\rangle \\ &= 2\frac{2g_L + \frac{1}{2}g_S(p^2-2)}{p^2+2} \\ &= 2\frac{p^2-4}{p^2+2} \\ &\approx -2.96. \end{aligned} \tag{5}$$

On the other hand, for the Cu^{2+} $3d^9$ or $t_{2g}^6e_g^3$ configuration, both $\mathbf{L}$ and spin-orbital coupling vanish. Thus,

$$g_{\mathrm{Cu}} = g_S = 2. \tag{6}$$

Therefore, the g factors on the Ir and Cu sites have opposite signs and different magnitudes.

III. ANALYSIS WITH THE ISING MODEL

To explore the essential effects of nonuniform g factors, we begin with the exactly solvable one-dimensional (1D) Ising model with alternating g factors. This model captures the essential physics of the quasi-1D Sr_3CuIrO_6 consisting of FM chains made up by alternating Cu (A-site) and Ir (B-site) ions [Fig. 1(d)]. Our exact solution features the zero-field susceptibility with both FM and AFM components, in agreement with the experiments. It also turns out that the system possesses an exotic magnetic-field-driven critical point (CP) [Fig. 1(e)] at which the spins with the smaller and larger magnitudes of g factors are fully disordered and ordered, respectively, at absolute zero temperature—reminiscent of the all-time favorite aesthetic concept of “half fire, half ice.”

The model is defined by the Hamiltonian

$$H = -J\sum_{i=1}^{N}\sigma_i\sigma_{i+1} - h\mu_B S\sum_{i=1}^{N}g_i\sigma_i, \tag{7}$$

which corresponds to N spins ($\sigma_i = \pm 1$) on a line with periodic boundary conditions $\sigma_{N+1} = \sigma_1$. h is a uniform longitudinal magnetic field. The g factors are alternating with $g_i = g_A$ for odd i and $g_i = g_B$ for even i. We solve the model exactly using the transfer matrix method [24] to calculate out the partition function and correlation functions (see Supplemental Material [27]).

The T-h phase diagram. The field h on the nonuniform g_A and g_B factors can be regarded as the superposition of the uniform field of magnitude of $h(g_A + g_B)/2$ and the staggered field of magnitude of $h(g_A - g_B)/2$ on a system with uniform $g \equiv 1$ factors. Therefore, in Fig. 2, we contrast the T-h dependencies of several thermodynamic quantities for the three cases: nonuniform $g_A = 2$ and $g_B = -3$ (the top row), staggered $g_A = -g_B = 2.5$ (the middle row, which is of the AFM type), and uniform $g_A = g_B = 0.5$ (the bottom row, which is of the FM type). Overall, the results for the $g_A = 2, g_B = -3$ case are FM-like in the low-h, low-T region, and they are AFM-like in the high-h region especially near the zero-temperature critical field h_c. Nevertheless, we notice two unusual features in the $g_A = 2$, $g_B = -3$ case. First, the low-h, high-T region is more AFM-like. The other is that $h_c = 2J/(\mu_B S g_A)$ depends on g_A, not on g_B. We elaborate the two anomalies below.

A. The zero-field limit: $h \to 0$

The initial susceptibility per site $\chi(h \to 0, T)$ takes the following elegant two-component form:

$$\frac{\chi(0,T)}{\mu_B^2 S^2} = \beta e^{2\beta J}\left(\frac{g_A+g_B}{2}\right)^2 + \beta e^{-2\beta J}\left(\frac{g_A-g_B}{2}\right)^2. \tag{8}$$

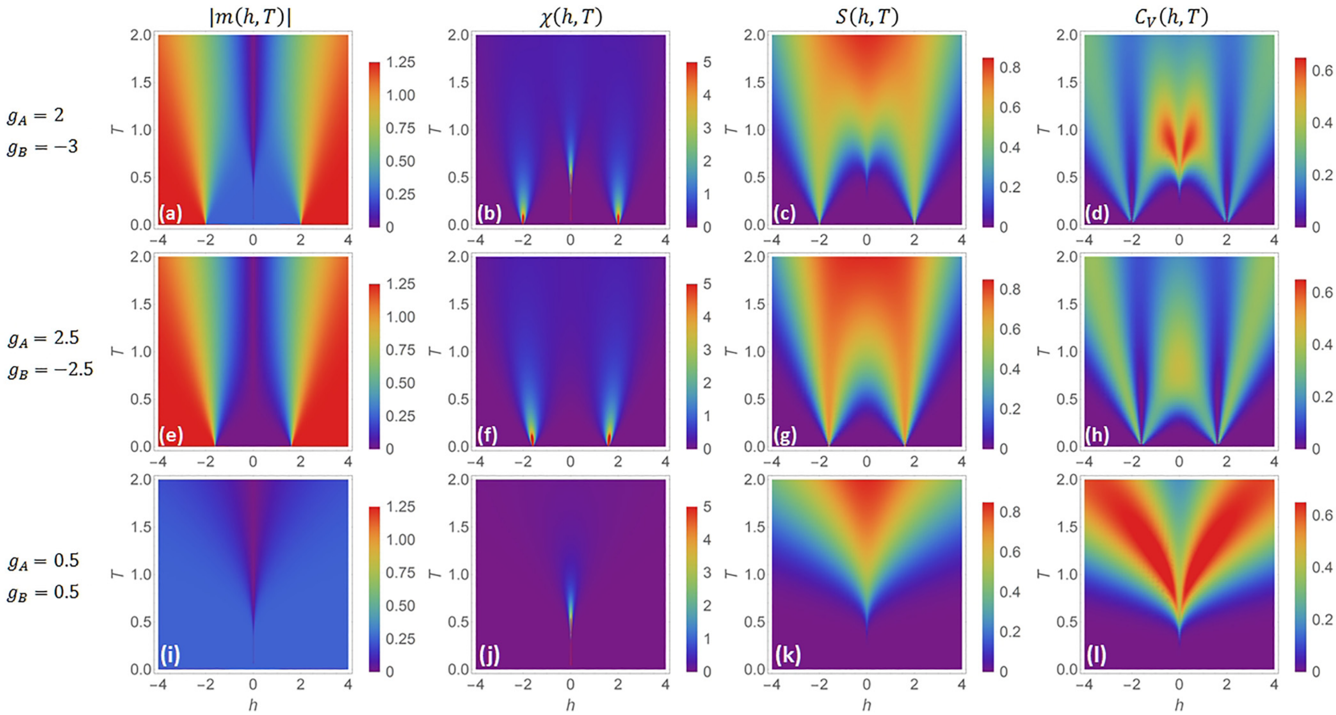

FIG. 2. Color maps of the T-h dependencies of the magnetization $|m(h,T)|$, the susceptibility $\chi(h,T)$, the entropy $S(h,T)/\ln 2$, and the specific heat $C_V(h,T)$ for the nonuniform (the top row), the uniform staggered (middle row), and the uniform (the bottom row) g factors.

The coexistence of the two components requires that g_A and g_B have different magnitude: $|g_A| \neq |g_B|$. Having exponents of opposite sign, the two components are of the FM and AFM types, respectively. Equation (8) is equivalent to the combined magnetic susceptibility of the FM chain with the uniform $g = (g_A + g_B)/2$ factors and the AFM chain with the uniform $g = (g_A - g_B)/2$ factors, which used to be called uniform and staggered susceptibilities, respectively [28]. The results for the realistic values of $g_A = 2$ and $g_B = -3$ in Sr_3CuIrO_6 are presented in Figs. 3(a) and 3(b). They agree qualitatively with the experimental results [15], indicating that the FM Ising chain model with such nonuniform g factors captures the essential physics of this copper-iridium oxide.

The spin frustration takes place when the two terms in Eq. (8) are comparable. As shown in Fig. 3(a), the FM term dominates at low T and the AFM one dominates at high T. The two terms become equal at

$$T_f = \frac{2J}{k_B}\left(\ln\left|\frac{g_A - g_B}{g_A + g_B}\right|\right)^{-1}. \tag{9}$$

The physical constraint of $T_f \geqslant 0$ requires [cf. Fig. 3(c)]

$$J g_A g_B < 0 \quad \text{and} \quad |g_A| \neq |g_B|. \tag{10}$$

Otherwise, for $J g_A g_B > 0$, $T_f < 0$ is unphysical [Fig. 3(c)]. Hence, to generate frustration in ferromagnets ($J > 0$), the g factors must have not only different magnitudes but also different signs.

To illustrate the effects of the requirement in Eq. (10), we present $\chi(0,T)$ for a variety of g_B/g_A [29] while fixing $J = 1$ in Fig. 3(d). For the cases of $g_B/g_A < 0$ (solid lines), $\chi(0,T)$ tends to dip down at an intermediate temperature near T_f, signaling the coexistence of comparable FM and AFM components. On the other hand, for the cases of $g_B/g_A > 0$ (dashed lines), the FM component dominates and

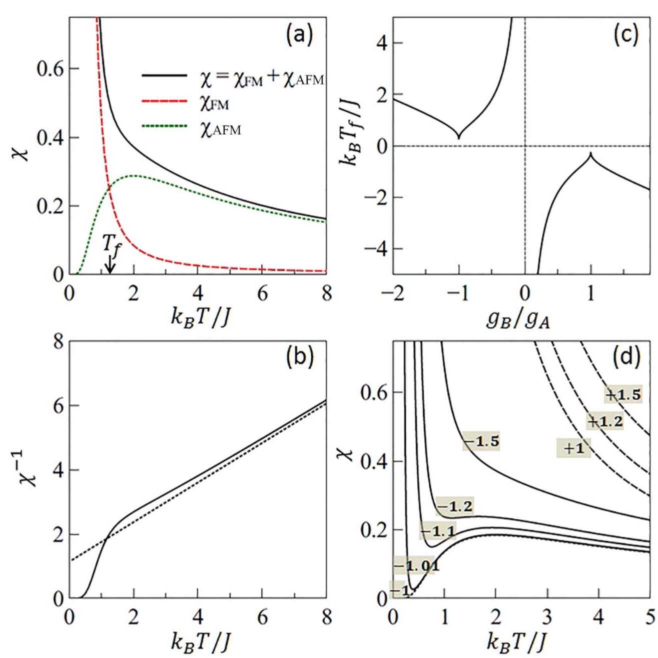

FIG. 3. The zero-field susceptibility (a) $\chi(0,T)$ (the black solid line). Its FM-like component χ_{FM} (the red dashed line) and the AFM-like component χ_{AFM} (the green dotted line) cross at T_f. (b) The inverse susceptibility χ^{-1} (the solid line). Its high-T Curie-Weiss behavior (the dotted line) wrongly suggests that the exchange interaction is AFM. $J = 1$, $g_A = 1$, and $g_B = -1.5$. (c) T_f as a function of g_B/g_A. (d) $\chi(0,T)$ for a variety of g_B/g_A (the numbers with the shaded background).

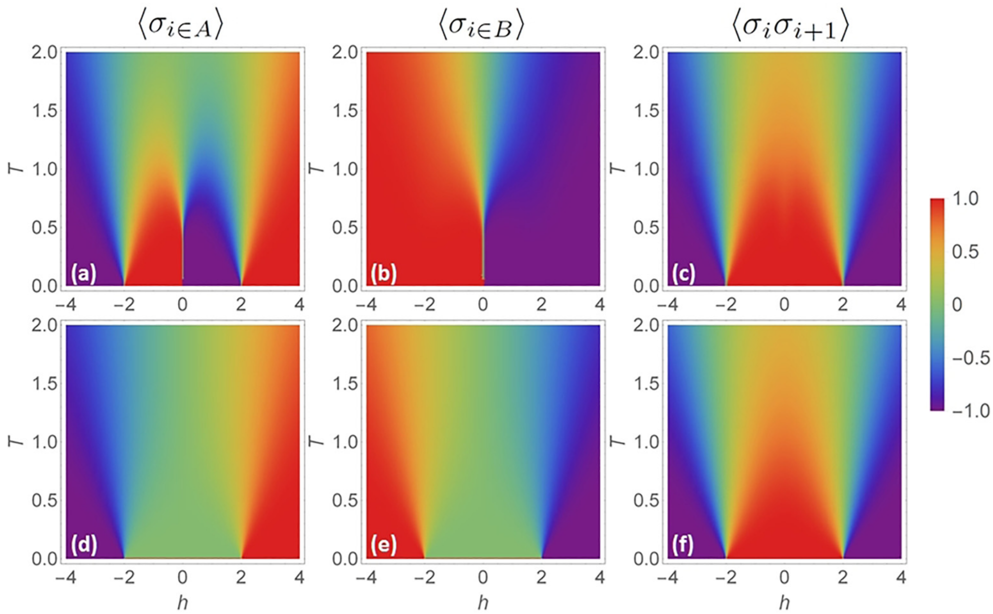

FIG. 4. Color maps of the T-h dependencies of the sublattice magnetization $\langle\sigma_{i\in A}\rangle$, $\langle\sigma_{i\in B}\rangle$, and the nearest-neighbor correlation function $\langle\sigma_i\sigma_{i+1}\rangle$ for the nonuniform g factors $g_A = 2$ and $g_B = -3$ (top row) and uniformly staggered g factors $g_A = -g_B = 2$ (bottom row). $J = 1$.

frustration vanishes. One may get the intuition for the requirement as follows. For FM $J > 0$, g_A and g_B have opposite signs; thus, sufficiently strong h will induce the AFM alignment of the spins, interfering with the FM J. Nevertheless, it is striking that the spin frustration takes place even at $h \to 0$.

The generic method for distinguishing the exchange interactions is to characterize the high-temperature behavior of the magnetic susceptibility using the Curie-Weiss form of $\chi = C/(T-\theta)$ with $\theta > 0$, $= 0$, and <0 corresponding to the FM, paramagnetic, and AFM types, respectively. Indeed, as shown in Fig. 3(b), the high-T expansion of Eq. (8) follows the Curie-Weiss law with

$$\theta = \frac{4J g_A g_B}{k_\mathrm{B}({g_A}^2 + {g_B}^2)}, \quad C = \mu_\mathrm{B}^2 S^2 \frac{g_A^2 + g_B^2}{2k_\mathrm{B}}. \tag{11}$$

The constraint $J g_A g_B < 0$ in Eq. (10) yields $\theta < 0$, which suggests the existence of an AFM exchange interaction [15]. However, this is a pure illusion.

B. At the critical field

Furthermore, we found that the zero-temperature CP at h_c in the present case of nonuniform g factors is qualitatively different from that in the usual case of $g_A = -g_B$. We analyze the $T = 0$ properties of the model Eq. (7) as a function of h. The magnetization per site is given by

$$\frac{m(h,0)}{\mu_\mathrm{B} S} = \begin{cases} (|g_B| - g_A)/2, & 0 < h < h_c, \\ |g_B|/2, & \text{for } h = h_c, \\ (|g_B| + g_A)/2, & h > h_c. \end{cases} \tag{12}$$

At the critical field $h_c = 2J/(\mu_\mathrm{B} S g_A)$, the magnetization is $\mu_\mathrm{B} S|g_B/2|$, which is independent of g_A. This means that the spins on the B sublattice are fully ordered, while the spins on the A sublattice do not contribute to the magnetization. Moreover, the entropy per site reads

$$S(h_c, 0) = \tfrac{1}{2} k_\mathrm{B} \ln 2. \tag{13}$$

Since the fully ordered spins on the B sublattice contribute nothing to the entropy, Eq. (13) means that the spins on the A sublattice are fully disordered, which would be usually imaged to occur at infinite temperature. Thus, the spins are said to be hotter than fire on the A sublattice but colder than ice on the B sublattice, as artistically illustrated in Fig. 1(e).

In comparison, the conventional Ising model with $J > 0$ and $-g_B = g_A = g$ has an equal contribution from the A and B sublattices by symmetry, yielding $m(h_c, 0)/\mu_\mathrm{B} S = g/\sqrt{5} \approx 0.447g$ and $S(h_c, 0) = k_\mathrm{B} \ln(\frac{1+\sqrt{5}}{2}) \approx 0.694 k_\mathrm{B} \ln 2$, which are not the $-g_B = g_A$ limit of Eqs. (12) and (13). The entropy is $0.347 k_\mathrm{B} \ln 2$ per sublattice, smaller than $0.5 k_\mathrm{B} \ln 2$, which means the two sublattices are still correlated in short ranges at the CP. Indeed, the correlation function $\langle\sigma_i\sigma_{i+1}\rangle = 1 - 2/\sqrt{5} \approx 0.106$ at the CP for $-g_B = g_A$ but it is zero for $-g_B > g_A$ (see Supplemental Material [27]). Therefore, the half fire, half ice phase is identified as a new phase.

More specifically, as shown in Fig. 4, for strong field $|h| > h_c$, both the normal and the present cases have a similar AFM spin configuration of $|+-+-\cdots\rangle$ at low T, which gains energy from the h term to overcome the energy cost from the J term. On the other hand, for weak field $|h| < h_c$, the normal case's ground state is degenerate with the FM $|++++\cdots\rangle$ and $|----\cdots\rangle$ spin configurations, exhibiting $\langle\sigma_{i\in A}\rangle = \langle\sigma_{i\in B}\rangle = 0$ and $\langle\sigma_i\sigma_{i+1}\rangle = 1$, which gains energy from the J term but nothing from the h term. This degeneracy due to the $g_A = -g_B$ symmetry is lifted by $g_A < -g_B$, yielding the single spin configuration of $|----\cdots\rangle$, which gains energy from both the J and h terms. The above distinct behaviors for $|h| < h_c$ lead to the distinct CP's at $|h| = h_c$: It is now the normal case that gains energy from both the J and h terms with $\langle\sigma_{i\in A}\rangle = -\langle\sigma_{i\in B}\rangle = 1/\sqrt{5}$ and $\langle\sigma_i\sigma_{i+1}\rangle \approx 0.106$, while the present case gains energy from the h term but nothing from the J term. Figure 4 (top panel) also clearly shows that the half fire, half ice state survives a wide temperature range near h_c.

Being a highly degenerate state the half fire, half ice CP strongly responds to perturbations, such as the transverse exchange interaction $-J_\perp \sum_i (S_i^x S_{i+1}^x + S_i^y S_{i+1}^y)$ known to be present in Sr_3CuIrO_6 [22]. At the CP, the B-sublattice spins are frozen in one direction and the A-sublattice spins are "paramagnetic." Thus, the A-sublattice spins can interact with each other via the virtual processes that flip the B-sublattice spins. Hence the vicinity of the CP is described by the effective XY model

$$H_{\mathrm{XY}} = \sum_{i\in A} \left[-J_{\mathrm{eff}}\left(S_i^x S_{i+2}^x + S_i^y S_{i+2}^y\right) - h_{\mathrm{eff}} S_i^z\right], \qquad (14)$$

where $J_{\mathrm{eff}} = J_\perp^2/2\Delta$ and $h_{\mathrm{eff}} = (h - h_c) g_A \mu_{\mathrm{B}} + J_\perp^2/4\Delta$ with $\Delta = |2h_c \mu_{\mathrm{B}} g_B S|$ being the energy cost to flip one B-sublattice spin. This model is exactly solvable by means of the Jordan-Wigner transformation which reduces it to the model of noninteracting fermions with the spectrum $\epsilon(k) = |h_{\mathrm{eff}}| - J_{\mathrm{eff}} \cos k$. Hence it remains quantum critical for $|h_{\mathrm{eff}}| < J_{\mathrm{eff}}$. The complete $J_\perp$-h phase diagram as well as the responses to other stimuli such as the transverse field will be published elsewhere.

IV. DISCUSSION

Nonuniform g factors have been of interest in the studies of magnetic crystals [28,30,31] and clusters [32], predominantly with pure $3d$ or pure $5d$ magnetic ions. The present exploration of the parameter space of $J g_A g_B < 0$ and $|g_A| \neq |g_B|$ is motivated by studying the mixed $3d$-$5d$ materials [22]. In particular, to see how unusual it is to reach the opposite signed g_A and g_B for FM $J > 0$, $g_A = g_B$ was assumed in previous studies of Sr_3CuIrO_6 [20,21]. We anticipate the understanding presented here to be widely relevant to other mixed $3d$-$5d$ transition-metal compounds, e.g., the "partial fire, partial ice" CP at which the spins with larger and smaller $|g_i|$ are frozen and boiling, respectively, in the other copper-iridium oxides [15–18].

Last but not least, the sign of J is not a prerequisite in the above analysis. With the constraint of $J g_A g_B < 0$, it is equally acceptable to have AFM $J < 0$ and $g_A g_B > 0$. This is achieved by the transformation $\sigma_i \to -\sigma_i$ for sites in the B sublattice only and the substitutions $J \to -J$ and $g_B \to -g_B$ in Eq. (7). Then, Eq. (8) was the same as Eq. (3.16) of Bell [33] or Eq. (3.2) of Bell [34]. However, Bell gave no more results for this model. Instead, Bell focused on the ferrimagnet with the A and B sites situated in the sequence $ABBABBABB\ldots$, as the arrangement of the Cu and Ir atoms in $Sr_4CuIr_2O_9$, yielding qualitatively similar results. Here, we were motivated by the recent studies of Sr_3CuIrO_6 to give a rather full account of the realistic model (7) and emphasize its role as a source of spin frustration. For ferrimagnets, the AFM exchange interaction implied by the high-T Curie-Weiss behavior is real, while the low-T response is FM-like. When the magnitudes of the g factors are similar [cf. the curve for $g_B/g_A = -1.01\%$ or -1.1% in Fig. 3(d)], $\chi(0, T)$ looks like the susceptibility of many antiferromagnets, which goes down as T decreases from the Néel temperature but mysteriously jumps up at very low T. The jump used to be attributed to the presence of magnetic impurity; the above results now offer an alternative mechanism. Most importantly, the analogous solution with the AFM exchange interaction greatly enlarges the range of materials containing nonuniform g-factor induced frustration.

V. SUMMARY

We have revealed magnetic frustration and an exotic "half fire, half ice" critical point in the Ising model with nonuniform g factors. We have shown that these unusual g-factor effects are essential to understanding the mixed copper-iridium oxides. Considering the wide range of applications of the Ising model, we anticipate to realize the frustration and "partial fire, partial ice" states in other systems as well.

ACKNOWLEDGMENTS

This work was supported by the U.S. Department of Energy (DOE), Office of Basic Energy Sciences (BES), the Materials Sciences and Engineering (MSE) Division under Contract No. DE-SC0012704. C.R.R. participated in the research via support from the Brookhaven National Laboratory Supplemental Undergraduate Research Program (SURP). We are grateful to Tiffany Bowman for helping illustrate Fig. 1(e).

[1] L. Balents, Spin liquids in frustrated magnets, Nature (London) **464**, 199 (2010).

[2] J. van den Brink, Z. Nussinov, and A. M. Oleś, Frustration in systems with orbital degrees of freedom, in *Introduction to Frustrated Magnetism*, edited by C. Lacroix, P. Mendels, and F. Mila (Springer, Berlin, Heidelberg, 2011), pp. 629–670.

[3] A. Kitaev, Anyons in an exactly solved model and beyond, Ann. Phys. **321**, 2 (2006).

[4] G. Jackeli and G. Khaliullin, Mott insulators in the strong spin-orbit coupling limit: From Heisenberg to a quantum compass and Kitaev models, Phys. Rev. Lett. **102**, 017205 (2009).

[5] G. Cao, H. Zheng, H. Zhao, Y. Ni, C. A. Pocs, Y. Zhang, F. Ye, C. Hoffmann, X. Wang, M. Lee, M. Hermele, and I. Kimchi, Quantum liquid from strange frustration in the trimer magnet $Ba_4Ir_3O_{10}$, npj Quantum Mater. **5**, 26 (2020).

[6] Y. Shen, J. Sears, G. Fabbris, A. Weichselbaum, W. Yin, H. Zhao, D. G. Mazzone, H. Miao, M. H. Upton, D. Casa, R. Acevedo-Esteves, C. Nelson, A. M. Barbour, C. Mazzoli, G. Cao, and M. P. M. Dean, Emergence of spinons in layered trimer iridate $Ba_4Ir_3O_{10}$, Phys. Rev. Lett. **129**, 207201 (2022).

[7] J. Strecka, Pseudo-critical behavior of spin-1/2 Ising diamond and tetrahedral chains, in *An Introduction to the Ising Model*, edited by S. Luoma (Nova Science Publishers, New York, 2020), pp. 63–86.

[8] T. Krokhmalskii, T. Hutak, O. Rojas, S. M. de Souza, and O. Derzhko, Towards low-temperature peculiarities of

thermodynamic quantities for decorated spin chains, Physica A **573**, 125986 (2021).
[9] A. Smerald and F. Mila, Disorder-driven spin-orbital liquid behavior in the $Ba_3xSb_2O_9$ materials, Phys. Rev. Lett. **115**, 147202 (2015).
[10] H. Yao and D.-H. Lee, Fermionic magnons, non-Abelian spinons, and the spin quantum Hall effect from an exactly solvable spin-1/2 Kitaev model with SU(2) symmetry, Phys. Rev. Lett. **107**, 087205 (2011).
[11] W. Yin, A paradigm of spontaneous marginal phase transition at finite temperature in one-dimensional ladder Ising models, arXiv:2006.08921.
[12] W. Yin, Finding and classifying an infinite number of cases of the marginal phase transition in one-dimensional Ising models, arXiv:2006.15087.
[13] T. Hutak, T. Krokhmalskii, O. Rojas, S. Martins de Souza, and O. Derzhko, Low-temperature thermodynamics of the two-leg ladder Ising model with trimer rungs: A mystery explained, Phys. Lett. A **387**, 127020 (2021).
[14] A. Weichselbaum, W. Yin, and A. M. Tsvelik, Dimerization and spin decoupling in a two-leg Heisenberg ladder with frustrated trimer rungs, Phys. Rev. B **103**, 125120 (2021).
[15] A. Niazi, P. L. Paulose, and E. V. Sampathkumaran, Inhomogeneous magnetism in single crystalline $Sr_3CuIrO_{6+\delta}$: Implications to phase-separation concepts, Phys. Rev. Lett. **88**, 107202 (2002).
[16] P. D. Battle, G. R. Blake, J. Darriet, J. G. Gore, and F. Weill, Modulated structure of $Ba_6ZnIr_4O_{15}$; a comparison with $Ba_6CuIr_4O_{15}$ and $SrMn_{1-x}Co_xO_{3-y}$, J. Mater. Chem. **7**, 1559 (1997).
[17] P. D. Battle, G. R. Blake, J. Sloan, and J. F. Vente, Commensurate and incommensurate phases in the system $A_4A'Ir_2O_9$ ($A =$ Sr, Ba; $A' =$ Cu, Zn), J. Solid State Chem. **136**, 103 (1998).
[18] G. R. Blake, J. Sloan, J. F. Vente, and P. D. Battle, Prediction and verification of the structural chemistry of new one-dimensional barium/copper/iridium oxides, Chem. Mater. **10**, 3536 (1998).
[19] T. N. Nguyen and H.-C. zur Loye, A family of one-dimensional oxides: Sr_3MIrO_6 ($M =$ Ni, Cu, Zn): Structure and magnetic properties, J. Solid State Chem. **117**, 300 (1995).
[20] T. N. Nguyen, P. A. Lee, and H.-C. Z. Loye, Design of a random quantum spin chain paramagnet: $Sr_3CuPt_{0.5}Ir_{0.5}O_6$, Science **271**, 489 (1996).
[21] A. Furusaki, M. Sigrist, P. A. Lee, K. Tanaka, and N. Nagaosa, Random exchange Heisenberg chain for classical and quantum spins, Phys. Rev. Lett. **73**, 2622 (1994).
[22] W.-G. Yin, X. Liu, A. M. Tsvelik, M. P. M. Dean, M. H. Upton, J. Kim, D. Casa, A. Said, T. Gog, T. F. Qi, G. Cao, and J. P. Hill, Ferromagnetic exchange anisotropy from antiferromagnetic superexchange in the mixed 3*d*-5*d* transition-metal compound Sr_3CuIrO_6, Phys. Rev. Lett. **111**, 057202 (2013).
[23] X. Liu, V. M. Katukuri, L. Hozoi, W.-G. Yin, M. P. M. Dean, M. H. Upton, J. Kim, D. Casa, A. Said, T. Gog, T. F. Qi, G. Cao, A. M. Tsvelik, J. van den Brink, and J. P. Hill, Testing the validity of the strong spin-orbit-coupling limit for octahedrally coordinated iridate compounds in a model system Sr_3CuIrO_6, Phys. Rev. Lett. **109**, 157401 (2012).
[24] D. C. Mattis and R. H. Swendsen, *Statistical Mechanics Made Simple* (World Scientific, Singapore, 2008).
[25] E. Schneidman, M. J. Berry II, R. Segev, and W. Bialek, Weak pairwise correlations imply strongly correlated network states in a neural population, Nature (London) **440**, 1007 (2006).
[26] J. Kanamori, Theory of the magnetic properties of ferrous and cobaltous oxides, I, Prog. Theor. Phys. **17**, 177 (1957).
[27] See Supplemental Material at http://link.aps.org/supplemental/10.1103/PhysRevB.109.054427 for technical details about the transfer matrix method used to calculate thermodynamical observables, correlation functions, and sublattice magnetization.
[28] M. Matsuura and Y. Ajiro, Crystallographic two sublattice system staggered susceptibility and induced staggered magnetization in paramagnetic state, J. Phys. Soc. Jpn. **41**, 44 (1976).
[29] It is adequate to discuss the case of $|g_B| \geqslant |g_A|$, since for $|g_B| \leqslant |g_A|$ one simply swaps the A and B labels to return to $|g_B| \geqslant |g_A|$.
[30] J. H. H. Perk, H. W. Capel, M. J. Zuilhof, and T. J. Siskens, On a soluble model of an antiferromagnetic chain with alternating interactions and magnetic moments, Physica A **81**, 319 (1975).
[31] M. Oshikawa and I. Affleck, Field-induced gap in $S = 1/2$ antiferromagnetic chains, Phys. Rev. Lett. **79**, 2883 (1997).
[32] V. Ohanyan, O. Rojas, J. Strečka, and S. Bellucci, Absence of actual plateaus in zero-temperature magnetization curves of quantum spin clusters and chains, Phys. Rev. B **92**, 214423 (2015).
[33] G. M. Bell, Ising ferrimagnetic models. I, J. Phys. C: Solid State Phys. **7**, 1174 (1974).
[34] G. M. Bell, Ising ferrimagnetic models. II, J. Phys. C: Solid State Phys. **7**, 1189 (1974).